Yeast phosphatidic acid phosphatase Pah1 hops and scoots along the membrane phospholipid bilayer

Joanna M. Kwiatek and George M. Carman[1]

Department of Food Science and Rutgers Center for Lipid Research, New Jersey Institute for Food, Nutrition, and Health, Rutgers University, New Brunswick, NJ 08901

ORCID ID: 0000-0003-4951-8233 (G.M.C.)

Abstract **PA phosphatase, encoded by *PAH1* in the yeast *Saccharomyces cerevisiae*, catalyzes the Mg^{2+}-dependent dephosphorylation of PA, producing DAG at the nuclear/ER membrane. This enzyme plays a major role in triacylglycerol synthesis and in the regulation of phospholipid synthesis. As an interfacial enzyme, PA phosphatase interacts with the membrane surface, binds its substrate, and catalyzes its reaction. The Triton X-100/PA-mixed micellar system has been utilized to examine the activity and regulation of yeast PA phosphatase. This system, however, does not resemble the in vivo environment of the membrane phospholipid bilayer. We developed an assay system that mimics the nuclear/ER membrane to assess PA phosphatase activity. PA was incorporated into unilamellar phospholipid vesicles (liposomes) composed of the major nuclear/ER membrane phospholipids, PC, PE, PI, and PS. We optimized this system to support enzyme-liposome interactions and to afford activity that is greater than that obtained with the aforementioned detergent system. Activity was regulated by phospholipid composition, whereas the enzyme's interaction with liposomes was insensitive to composition. Greater activity was attained with large (≥100 nm) versus small (50 nm) vesicles. The fatty-acyl moiety of PA had no effect on this activity. PA phosphatase activity was dependent on the bulk (hopping mode) and surface (scooting mode) concentrations of PA, suggesting a mechanism by which the enzyme operates along the nuclear/ER membrane in vivo.**—Kwiatek, J. M., and G. M. Carman. **Yeast phosphatidic acid phosphatase Pah1 hops and scoots along the membrane phospholipid bilayer. *J. Lipid Res.* 2020.** 61: **1232–1243.**

Supplementary key words lipin • phosphatidate • diacylglycerol • triacylglycerol • phospholipid vesicle • liposome • interfacial enzyme kinetics • Nem1-Spo7 protein phosphatase • lipid metabolism

PA phosphatase (3-*sn*-phosphatidate phosphohydrolase, EC 3.1.3.4), which is encoded by the *PAH1* gene in the yeast *Saccharomyces cerevisiae* (1),[2] catalyzes the Mg^{2+}-dependent dephosphorylation of PA to produce DAG (**Fig. 1**) (2, 3). PA phosphatase has emerged as one of the most important lipid metabolic enzymes because it largely controls whether cells synthesize membrane phospholipids or the neutral lipid triacylglycerol (TAG) (4–6). The substrate PA is the direct precursor of the liponucleotide CDP-DAG that is converted to all membrane phospholipids (6–12), whereas the product DAG is the direct precursor of TAG (Fig. 1) (6, 13–19). The DAG produced in the reaction may also be used for the synthesis of the phospholipids PC and/or PE via the CDP-choline and/or CDP-ethanolamine branches of the Kennedy pathway (20–24) if cells are supplemented with choline and/or ethanolamine (Fig. 1) (25, 26). This DAG-dependent alternative pathway is essential for cells with a loss-of-function mutation in the CDP-DAG-dependent synthesis of PS, PE, or PC; these mutants are auxotrophic for choline and/or ethanolamine, indeed (27–31). The substrate and product of the PA phosphatase also have important signaling functions in cells. For example, PA has a strong influence on the Opi1-mediated transcriptional regulation of UAS_{INO}-containing phospholipid synthesis gene expression (6, 12, 32–35), whereas DAG, along with PS, is required for the phosphorylation of lipid metabolic enzymes by protein kinase C (36).

As one might expect of cells lacking an enzyme that controls important lipid metabolic intermediates, the *pah1*Δ mutant exhibits phenotypes indicative of major defects in lipid metabolism and cell physiology (6). Notable defects include a reduction in the formation of TAG (1, 37) and lipid droplets (38, 39), a susceptibility to fatty acid-induced lipotoxicity (39) and oxidative stress (40), elevated levels of PA and the abnormal expansion of the nuclear/ER membrane (32, 41–43), defects in vacuole fusion (44–46) and TORC1-mediated induction of autophagy (46), loss of cell wall integrity (47, 48), and inability to grow at elevated (1, 32, 49) or reduced (50) temperatures and to utilize glycerol

This work was supported, in whole or in part, by National Institutes of Health United States Public Health Service Grants GM028140 and GM136128. The content is solely the responsibility of the authors and does not necessarily represent the official views of the National Institutes of Health. The authors declare that they have no conflicts of interest with the contents of this article.

Manuscript received 26 May 2020 and in revised form 9 June 2020.

Published, JLR Papers in Press, June 15, 2020
DOI https://doi.org/10.1194/jlr.RA120000937

[1] To whom correspondence should be addressed.
e-mail: gcarman@rutgers.edu

[2] Yeast *PAH1*-encoded PA phosphatase is also known as Pah1. The term yeast is used interchangeably with *S. cerevisiae*.

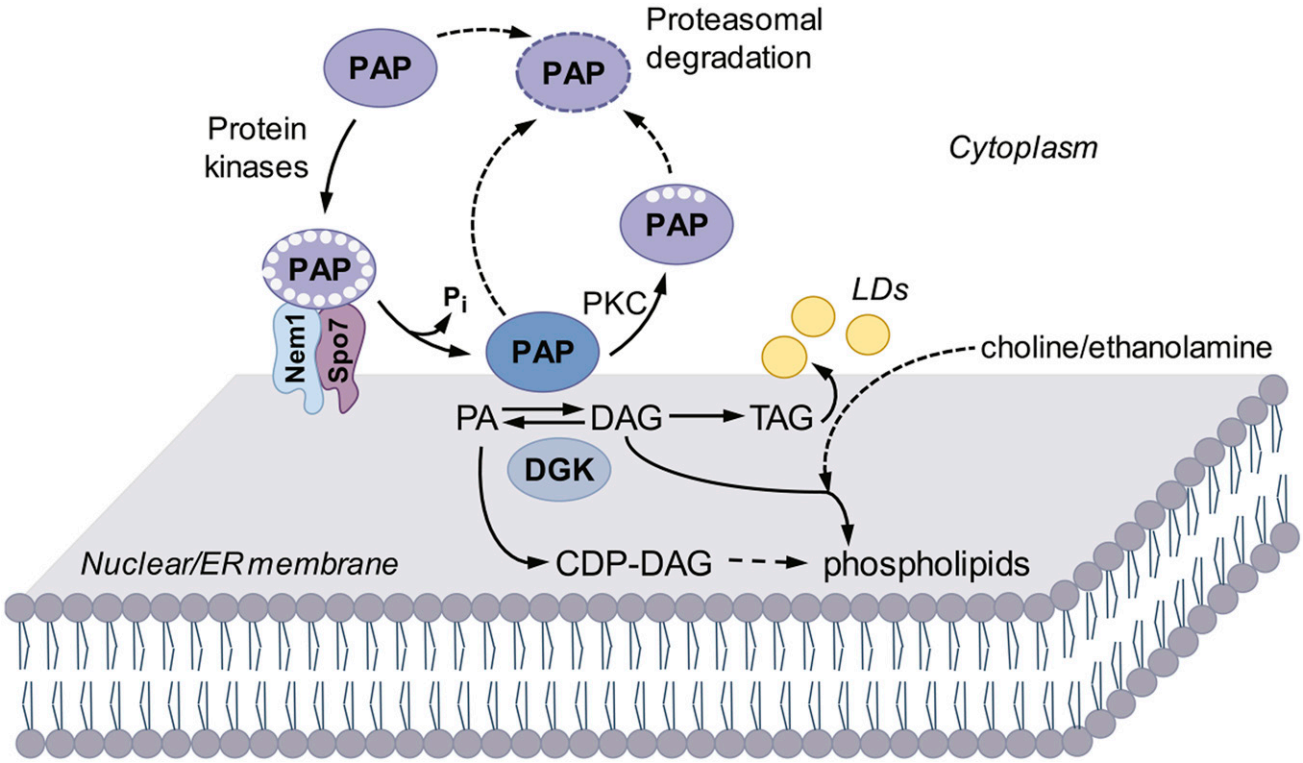

Fig. 1. Model for the regulation of Pah1 PA phosphatase (PAP) localization and stability by phosphorylation and dephosphorylation, and the role of PA phosphatase in lipid synthesis. PA phosphatase is phosphorylated (small white circles) by multiple protein kinases in the cytoplasm; the phosphorylated enzyme translocates to the nuclear/ER membrane through its dephosphorylation by the Nem1-Spo7 complex. Dephosphorylated PA phosphatase that is associated with the nuclear/ER membrane catalyzes the conversion of PA to DAG, which is converted to TAG for storage in lipid droplets (*LDs*). The PA phosphatase molecule catalyzing the dephosphorylation of PA is denoted with blue color. The DAG produced in the PA phosphatase reaction may be converted to the phospholipids PC and/or PE via the Kennedy pathway if cells are supplemented with choline and/or ethanolamine. DAG may be converted to PA by the CTP-dependent DAG kinase (DGK) reaction. The PA phosphatase substrate PA is used for the synthesis of the major ER membrane phospholipids (PC, PE, PI, PS) via CDP-DAG. The unphosphorylated/dephosphorylated forms of PA phosphatase or protein kinase C (PKC)-phosphorylated PA phosphatase are degraded by the 20S proteasome (indicated by the dashed line arrows). More comprehensive descriptions of the lipid synthetic pathways and the regulation of PA phosphatase may be found elsewhere (5, 6, 11, 12).

as a carbon source (1, 42). Overall, the *pah1*Δ mutant exhibits a shortened chronological life span (40) with apoptotic cell death in the stationary phase (39). The mutant phenotypes that are ascribed to elevated PA content (6) can also be shown in wild-type cells by the overexpression of Dgk1 DAG kinase, which catalyzes the CTP-dependent conversion of DAG to PA (Fig. 1) (51, 52).

The PA phosphatase (also known as lipin)[3] is conserved in higher eukaryotes including mice (53, 54) and humans (1, 53, 55). Loss of lipin PA phosphatase activity results in a plethora of lipid-based syndromes that include lipodystrophy, insulin resistance, rhabdomyolysis, myoglobinuria, inflammatory disorders, peripheral neuropathy, and the Majeed and metabolic syndromes (53, 56–61).

Studies aimed at understanding the regulation and mode of action of PA phosphatase have been subject to intense investigations (5, 62). In a current working model for the regulation of yeast Pah1 PA phosphatase (Fig. 1), the enzyme is phosphorylated in the cytoplasm by multiple protein kinases (63–68). This posttranslational modification inhibits the PA phosphatase function by causing its retention in the cytoplasm apart from its substrate that resides in the nuclear/ER membrane (63–66, 69). Phosphorylated PA phosphatase is then recruited to the membrane through its association and dephosphorylation by the Nem1-Spo7 protein phosphatase complex (32, 41, 70). The dephosphorylated PA phosphatase associates with the membrane via its amphipathic helix, binds its substrate PA, and then catalyzes the conversion of PA to DAG (1, 5, 6, 70, 71). Additionally, the phosphorylation of PA phosphatase attenuates its activity, whereas the dephosphorylation stimulates its activity (64, 65, 69, 72). The unphosphorylated/dephosphorylated or protein kinase C-phosphorylated PA phosphatase is liable to degradation by the 20S proteasome (73, 74).

PA phosphatase is an interfacial enzyme; it interacts with the membrane surface, binds its substrate, and then catalyzes the production of DAG. The detergent/phospholipid-mixed micelle system has facilitated the kinetic analyses of

[3]The mouse and human forms of PA phosphatase, which are encoded by the *Lpin1*, *-2*, and *-3* and *LPIN1*, *-2*, and *-3* genes, respectively, are also known as lipin (53, 54).

several interfacial phospholipid synthetic (75–80) and degrading (81–92) enzymes. The in vitro assay to measure yeast PA phosphatase activity has been performed with PA solubilized in the detergent Triton X-100 (1, 93–96). Triton X-100 forms a uniform mixed micelle with PA, providing a surface for catalysis (93). The detergent micelle system has permitted defined studies on the kinetics of the PA phosphatase reaction (1, 93) as well as on the biochemical regulation of the enzyme by phospholipids (96), sphingolipids (94), nucleotides (95), and by phosphorylation (64–66, 68). Although the Triton X-100/PA-mixed micelle assay allows for defined activity measurements, it does not resemble the in vivo environment of phospholipid bilayer membrane where PA is a component. Accordingly, we sought to establish an assay condition that mimics the in vivo environment of the nuclear/ER membrane in measuring PA phosphatase activity. PA was incorporated into unilamellar vesicles (liposomes) composed of the major ER membrane phospholipids, PC, PE, PI, and PS. This liposome system supported the interaction of PA phosphatase with the membrane and afforded the enzyme activity greater to that observed in the Triton X-100/PA-mixed micelle assay. Moreover, PA phosphatase catalyzed its reaction in the hopping and scooting modes, implicating how the enzyme operates along the nuclear/ER membrane in vivo.

MATERIALS AND METHODS

Materials

Avanti Polar Lipids was the source of soybean PI, dioleoyl derivatives of PC, PE, PS, and PA, other fatty-acyl derivatives of PA, and the polycarbonate filters used to prepare liposomes. Coomassie Blue R-250, molecular mass protein standards, and reagents for electrophoresis, immunoblotting, and protein assay were purchased from Bio-Rad. Malachite green was purchased from Fisher Scientific. GE Healthcare was the supplier of polyvinylidene difluoride paper and the enhanced chemifluorescence Western blotting detection kit. Millipore Sigma was the source of ammonium molybdate, BSA, and Triton X-100. The alkaline phosphatase-conjugated goat anti-rabbit IgG antibody was a product of Thermo Scientific. All other chemicals were reagent grade or better.

Preparation of purified Pah1

Escherichia coli-expressed His_6-tagged yeast Pah1 was purified from bacterial cell extracts by affinity chromatography with nickel-nitrilotriacetic acid-agarose as described by Han, Wu, and Carman (1). The protein content of enzyme preparations was estimated by the method of Bradford (97) using BSA as a standard. SDS-PAGE (98) analysis indicated that the Pah1 preparation was highly purified.

Preparation of liposomes

Liposomes (unilamellar phospholipid vesicles) were prepared by the extrusion method of MacDonald et al. (99) using an Avanti mini-extruder. Unless otherwise indicated, the dioleoyl derivatives of PC, PE, PS, PA, and soybean PI were used in this work. Chloroform was evaporated from the phospholipid mixtures under a stream of nitrogen to form a thin film, and residual solvent was removed in vacuo. Phospholipids were then resuspended in 20 mM Tris-HCl (pH 7.5) to a final concentration of 20 mM. After five cycles of freezing and thawing, the phospholipid suspensions were repeatedly extruded through a polycarbonate filter to produce vesicles with diameters of 51.3 ± 2.5 nm, 101.3 ± 2.5 nm, or 299.3 ± 3.7 nm. A Brookhaven Instruments particle size analyzer was used to confirm the size of liposomes. Under most conditions used in this study, the liposomes were made of PC/PE/PI/PS/PA (33.75:22.5:22.5:11.25:10 mol%). Additional liposomes were made of PC/PA (90:10 mol%), PC/PE/PA (60:30:10 mol%), PC/PS/PA (60:30:10 mol%), PC/PI/PA (60:30:10 mol%), PC/PE/PS/PA (45:30:15:10 mol%), PC/PE/PI/PS (45:30:15:10 mol%). The molar percent of PA in the liposome comprised of PC/PE/PI/PS/PA was calculated using the following formula, $mol\%_{PA}$ = [PA (molar)]/[PA (molar) + PC (molar) + PE (molar) + PI (molar) + PS (molar)] × 100.

Preparation of Triton X-100/PA-mixed micelles

PA in chloroform was transferred to a test tube and solvent was removed with a stream of nitrogen; residue solvent was removed in vacuo. Uniform Triton X-100/PA-mixed micelles (90:10 mol%) were prepared by adding Triton X-100 to the dried PA (93). The molar percent of PA in the Triton X-100/PA-mixed micelles was calculated using the following formula, $mol\%_{PA}$ = [PA (molar)]/[PA (molar) + Triton X-100 (molar)] × 100.

Pah1-liposome interaction assay

Pah1 was incubated for 15 min with the indicated liposomes in 20 mM Tris-HCl (pH 7.5) buffer containing 150 mM NaCl in a total volume of 30 μl at 30°C. Following incubation, the reaction mixture was subjected to centrifugation at 100,000 *g* for 1 h at 4°C, and the liposome pellet was resuspended in the same volume as the supernatant. Samples (20 μl) of each fraction were separated by SDS-PAGE (98), followed by immunoblotting (100–102) with polyvinylidene difluoride membrane using rabbit anti-Pah1 antibody (63). Anti-Pah1 antibody was used at a final concentration of 2 μg/ml. The goat anti-rabbit IgG antibody conjugated with alkaline phosphatase was used at a dilution of 1:4,000. Immune complexes were detected using the enhanced chemifluorescence immunoblotting substrate. Fluorimaging, using a Storm 865 molecular imager (GE Healthcare) was used to acquire fluorescence signals from immunoblots, and the intensities of the images were analyzed by ImageQuant TL software (GE Healthcare). A standard curve was used to ensure that the immunoblot signals were in the linear range of detection.

PA phosphatase assay

PA phosphatase activity was measured at 30°C for 15 min by following the release of water-soluble P_i from chloroform-soluble PA; the P_i produced in the reaction was measured with malachite green-molybdate reagent (55, 103). The reaction mixture contained 50 mM Tris-HCl (pH 7.5), 1 mM $MgCl_2$, enzyme protein, and the PA-containing liposomes in a final volume of 10 μl. The molar ratio of PC/PE/PI/PS to PA was 9:1 (10 mol% PA). Alternatively, the PA phosphatase activity was measured with the Triton X-100/PA-mixed micelle as the substrate; the molar ratio of Triton X-100 to PA was 9:1 (10 mol% PA) (1). Enzyme assays were conducted in triplicate, and the average SD of the assays was ±5%. All enzyme reactions were linear with time and protein concentration. A unit of enzymatic activity was defined as the amount of enzyme that catalyzed the formation of 1 nmol of product per minute.

Data analysis

The enzyme kinetics module of SigmaPlot software was used to analyze kinetic data according to Michaelis-Menten and Hill equations. Microsoft Excel software was used for the statistical analysis of the data. The *P* values <0.05 were taken as a significant difference.

Rationale

In establishing a liposome model for PA phosphatase assay, we took advantage of the fact that the requirement of the Nem1-Spo7 complex for the dephosphorylation and membrane interaction of the enzyme is circumvented by its phosphorylation-deficient form (32, 63, 69, 70, 104). Moreover, phosphorylation decreases the interaction of PA phosphatase with simple PC/PA liposomes (104). Accordingly, we utilized the *E. coli*-expressed form of Pah1 (1), which is free of phosphorylation that occurs when the enzyme is expressed in yeast (69). Liposomes were prepared from PC, PE, PI, PS, and PA to mimic the phospholipid composition of the nuclear/ER membrane found in yeast (105–107). The amount of PA (10 mol%) used in the liposomes is a saturating surface concentration as determined from this work (see below, Fig. 9). The average diameter of the liposomes used in this study was 100 nm unless otherwise indicated, which is a typical size for large unilamellar vesicles (99). The fidelity of the Pah1 was assessed by the measurement of its PA phosphatase activity using the established Triton X-100/PA-mixed micellar assay (108).

Effect of phospholipid composition on the interaction of Pah1 with liposomes

We examined an optimal amount of Pah1 for its liposomal interaction using a saturating amount of liposomes (see below, Fig. 5) containing PC/PE/PI/PS/PA (**Fig. 2**). The divalent cation Mg^{2+}, which is required for PA phosphatase activity (1, 3) but has no effect on the interaction of the enzyme with PC/PA liposomes (104), was omitted in the binding assay to prevent the dephosphorylation of PA; the presence of PA has an effect on the liposome interaction (104) (see below, Fig. 3). Most Pah1 bound to the liposomes when 37.5 ng of protein was used for the assay. The increasing amounts of Pah1 led to the saturation of the liposomes with a concomitant increase in the amount of unbound protein. Owing that 90% Pah1 was associated with the liposomes using 75 ng of protein and this amount was within the linear range for measuring PA phosphatase activity (see below), 75-80 ng protein was used in subsequent binding and PA phosphatase activity measurements.

In the next set of experiments, we questioned what effect the phospholipid composition would have on the interaction of Pah1 with liposomes (**Fig. 3**). Fifty-seven percent Pah1 associated with liposomes composed of PC/PE/PI/PS. The presence of 10 mol% PA in the liposomes showed a 1.6-fold increase in the enzyme association. This result is consistent with a previous finding with liposomes composed of PC and PC/PA (104). The effect of phospholipid composition on the interaction of Pah1 with the PA-containing liposomes was examined further. The different types of liposomes contained the major phospholipid PC and the substrate PA, but differed in the level and composition of the phospholipids PE, PI, and PS. In general, the phospholipid composition of PA-containing liposomes did not have a major effect on the interaction of Pah1 with liposomes (Fig. 3).

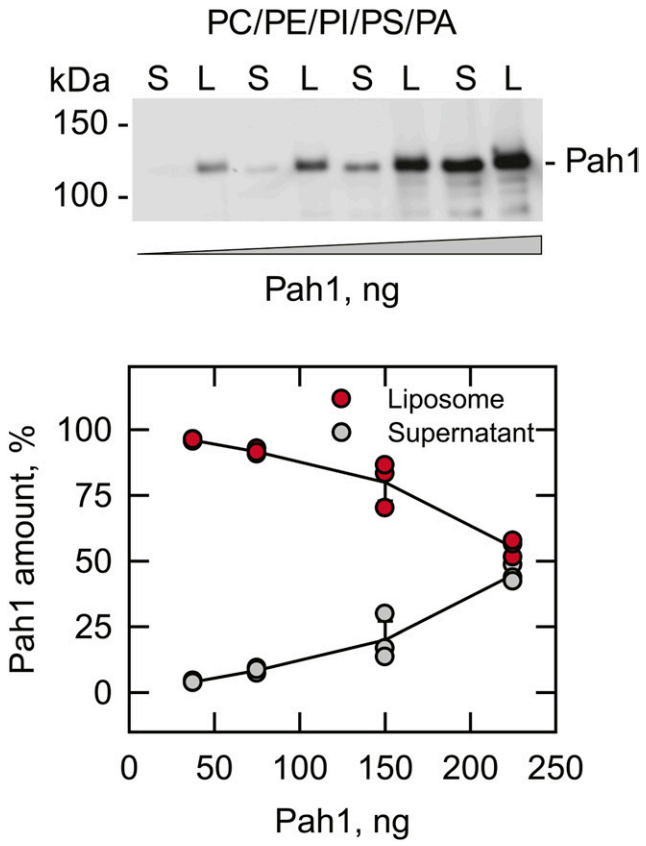

Fig. 2. Effect of Pah1 amount on the interaction with liposomes composed of PC/PE/PI/PS/PA. The indicated amounts of Pah1 were incubated with liposomes composed of PC/PE/PI/PS/PA. Following a 15 min incubation at 30°C, liposomes were collected by centrifugation at 100,000 *g* for 1 h at 4°C. The liposome (L) fraction was suspended in buffer to the same volume as that of the supernatant (S) fraction and equal volumes of each fraction were subjected to SDS-PAGE followed by immunoblot analysis with anti-Pah1 antibody. Upper panel: The immunoblot shown is representative of three experiments. The positions of Pah1 and molecular mass standards are indicated. Lower panel: The relative amounts of Pah1 associated with the liposome and supernatant fractions shown in the upper panel were quantified by ImageQuant software. The graph shows the individual data points for the three experiments. The lines represent the averages ± SD (error bars) of the three data points. Error bars are hidden behind some symbols.

Effect of phospholipid composition on the Pah1 PA phosphatase activity with liposomes

We confirmed the fidelity of the Pah1 enzyme preparation by the measurement of PA phosphatase activity using the established Triton X-100/PA-mixed micelle assay (108). To compare Triton X-100/PA-mixed micelles with the PA-containing liposomes in the enzyme assay, the level of PA was maintained at the saturating surface concentration of 10 mol% (93). As described previously (104), the PA phosphatase activity on PC/PA liposomes was 20% of the activity observed with Triton X-100/PA-mixed micelles (**Fig. 4**). However, when the liposomes contained the PC/PE/PI/PS/PA mixture resembling the phospholipid composition of the yeast ER membrane (105–107), the PA phosphatase activity was 1.4-fold higher than that measured with the Triton X-100/PA-mixed micelle (Fig. 4).

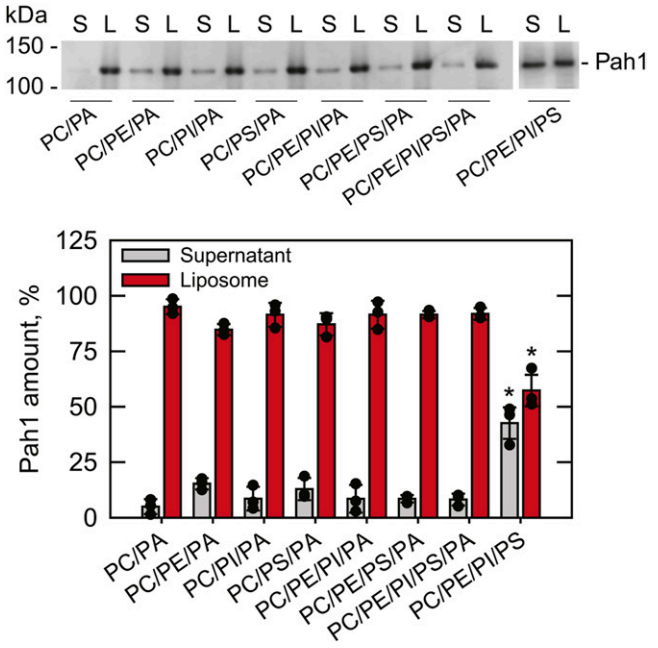

Fig. 3. Effect of phospholipid composition on the interaction of Pah1 PA phosphatase with liposomes. Pah1 (75 ng) was incubated with the indicated liposomes. The surface concentration of PA within each type of liposome was 10 mol%. Following a 15 min incubation at 30°C, liposomes were collected by centrifugation at 100,000 *g* for 1 h at 4°C. The liposome (L) fraction was suspended in buffer to the same volume as that of the supernatant (S) fraction and equal volumes of each fraction were subjected to SDS-PAGE followed by immunoblot analysis with anti-Pah1 antibody. Upper panel: The immunoblot shown is representative of three experiments. The positions of Pah1 and molecular mass standards are indicated. Lower panel: The relative amounts of Pah1 associated with the liposome and supernatant fractions were quantified by ImageQuant software. The data shown are the averages of the three experiments ± SD (error bars). The individual data points are also shown. $*P < 0.05$ versus the amounts with the PC/PE/PI/PS/PA liposomes.

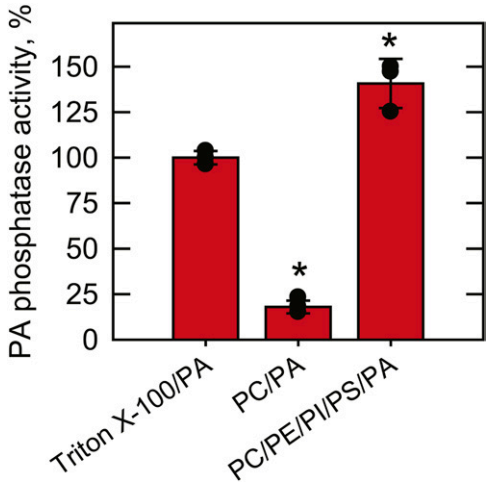

Fig. 4. Pah1 PA phosphatase activity using Triton X-100/PA-mixed micelles and phospholipid/PA liposomes. Pah1 (80 ng) was assayed (15 min) for PA phosphatase activity by following the release of P_i from PA using saturating amounts of Triton X-100/PA-mixed micelles (93) or phospholipid/PA liposomes. The surface concentration of PA within the detergent micelles or liposomes was 10 mol%. The activity using the Triton X-100/PA-mixed micelles (900 nmol/min/mg) was arbitrarily set at 100%. The data shown are the averages of the three experiments ± SD (error bars). The individual data points are also shown. $*P < 0.05$ versus the PA phosphatase activity with Triton X-100/PA-mixed micelles.

To examine the dependence of PA phosphatase on liposome composition in more detail, the activity was measured with liposomes composed of the major phospholipids in different combinations (**Fig. 5**). For each combination, the PA surface concentration was maintained at 10 mol%. The PA phosphatase activity observed for each liposome composition was dependent on the PA molar concentration (e.g., liposome amount). Greatest activity was observed using liposomes composed of complex mixtures of the phospholipids. On the one hand, the V_{max} with liposomes composed of PC/PE/PS/PA (2,300 nmol/min/mg) or PC/PE/PI/PA (2,500 nmol/min/mg) was 1.6- to 1.7-fold greater than that observed with liposomes composed of PC/PE/PI/PS/PA (1,400 nmol/min/mg). On the other hand, the K_m value for PA with the liposomes composed of PC/PE/PI/PS/PA (0.32 mM) was 1.8-fold less than that for the liposomes made of PC/PE/PS/PA (0.59 mM) or PC/PE/PI/PA (0.58 mM). Yet based on the specificity constant (V_{max}/K_m) (109) values (3,900-4,300 nmol/min^{-1}/mg^{-1}/mM^{-1}), all three liposome compositions were equally good in supporting PA phosphatase activity. The liposomes composed of PC/PE/PI/PS/PA more closely mimic the nuclear/ER membrane composition and thus were routinely used in this work.

We considered that the fatty-acyl moiety of PA might affect the PA phosphatase activity on the liposomes composed of PC/PE/PI/PS/PA (**Fig. 6**). In wild-type yeast, about 50% of PA contains 16:0 at the *sn*-1 position and 18:1 at the *sn*-2 position (39). The activity observed with this fatty-acyl composition was not majorly different from that observed with the dioleoyl derivative of PA routinely used in this study. Additionally, the variety of fatty-acyl compositions of

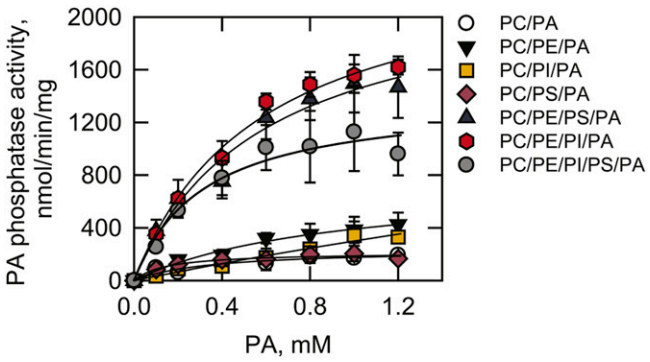

Fig. 5. Effect of phospholipid composition on the Pah1 PA phosphatase activity with liposomes. Pah1 (80 ng) was assayed (15 min) for PA phosphatase activity by following the release of P_i from PA using the indicated liposomes. The surface concentration of PA within each type of liposome was 10 mol%. The molar concentration of PA was varied by the addition of increasing amounts of liposomes. The data points represent the average of three experiments ± SD (error bars). The best-fit curves are the result of a Michaelis-Menten analysis of the data using the Enzyme Kinetics module of SigmaPlot software.

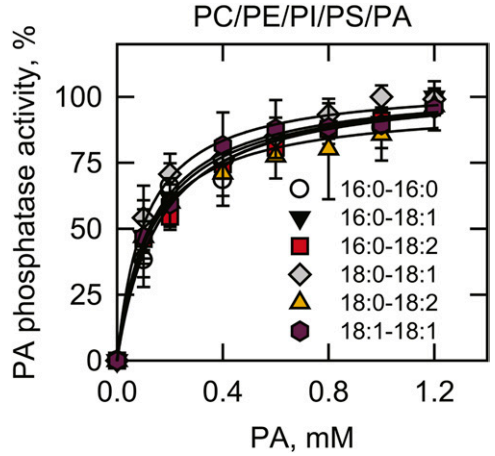

Fig. 6. Effect of fatty-acyl moiety composition of PA on Pah1 PA phosphatase activity using liposomes composed of PC/PE/PI/PS/PA. Pah1 (80 ng) was assayed (15 min) for PA phosphatase activity by following the release of P_i from the indicated PA molecular species using liposomes composed of PC/PE/PI/PS/PA. The surface concentration of PA within the liposomes was 10 mol%. The concentration of PA was varied by the addition of increasing amounts of liposomes. The data points represent the average of three experiments ± SD (error bars). The best-fit curves are the result of a Michaelis-Menten analysis of the data using the Enzyme Kinetics module of SigmaPlot software.

the PA had little effect on the PA phosphatase activity using the liposomes made of PC/PE/PI/PS/PA (Fig. 6).

The liposomes used in this work were 100 nm in diameter, a size widely used for large unilamellar vesicles (99). We considered whether smaller (50 nm) or larger (300 nm) size liposomes would impact on the PA phosphatase activity (**Fig. 7**). At a saturating amount of liposomes at 1 mM PA, the activity observed with the 100 nm liposomes was 2-fold higher when compared with the activity of the 50 nm liposomes. However, the increase of liposome size

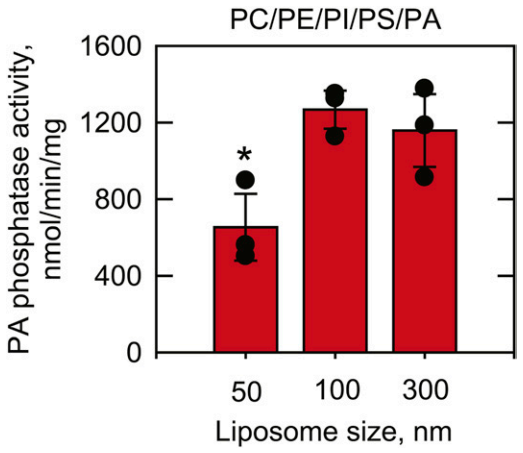

Fig. 7. Effect of liposome size on Pah1 PA phosphatase activity. Pah1 (80 ng) was assayed (15 min) for PA phosphatase activity by following the release of P_i from PA using the indicated liposome size composed of PC/PE/PI/PS/PA. The surface concentration of PA within the liposomes was 10 mol%. The data shown are the averages of the three experiments ± SD (error bars). The individual data points are also shown. $*P < 0.05$ versus the PA phosphatase activity with 100 nm liposomes.

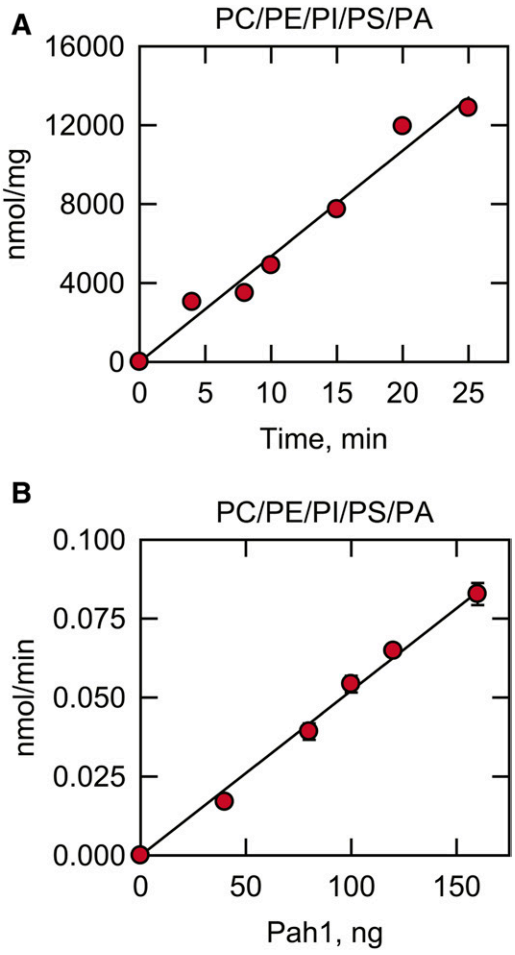

Fig. 8. Dependence of Pah1 PA phosphatase activity on time and Pah1 content using liposomes composed of PC/PE/PI/PS/PA. Pah1 was assayed for PA phosphatase activity by following the release of P_i from PA using liposomes composed of PC/PE/PI/PS/PA. The surface concentration of PA within the liposomes was 10 mol%. The enzyme activity was measured for the indicated time intervals (A) with 80 ng Pah1 or for 15 min with the indicated amounts of Pah1 (B). The data shown are the mean ± SD (error bars) from triplicate enzyme determinations. Error bars are hidden behind the symbols.

to 300 nm had no effect on increasing the enzyme activity observed with the 100 nm liposomes.

Having characterized the liposome system in terms of phospholipid composition, we set forth to demonstrate that the PA phosphatase reaction is linear with time and the amount of Pah1 (**Fig. 8**). That the activity was linear with time and protein indicates that the reaction follows zero order kinetics with respect to PA within the liposome. Based on the results of these experiments, the routine assays for measuring PA phosphatase activity with the liposomes composed of PC/PE/PI/PS/PA were conducted for 15 min with 80 ng enzyme.

Dependence of Pah1 PA phosphatase activity on the surface concentration of PA in liposomes

Peripheral membrane enzymes such as Pah1 PA phosphatase (1, 93) act in a cellular environment in which both three-dimensional bulk interactions (e.g., hopping mode)

JOURNAL OF LIPID RESEARCH ASBMB

occur at an aqueous-membrane interface and two-dimensional surface interactions (e.g., scooting mode) occur at the membrane bilayer (110, 111) (see below, Fig. 10). The data shown in Fig. 5 demonstrated that PA phosphatase activity was dependent on the molar concentration of PA (liposome amount), and thus functions in the hopping mode using the liposome system. We next set forth to demonstrate that the activity is dependent on the surface concentration of PA, and thus, functions in the scooting mode. For the experiment shown in **Fig. 9**, eight types of liposomes were prepared; in each liposome type, the molar ratio of PC/PE/PI/PS was maintained at 33.75:22.5:22.5:11.25 mol% to mimic the yeast nuclear/ER membrane, and the molar ratio of the combined phospholipid mixture to PA was varied to achieve the indicated surface concentrations of PA. Under the conditions of this experiment, the PA phosphatase activity was measured with a saturating amount of liposomes (1 mM PA). The kinetic data were analyzed according to the Michaelis-Menten and Hill equations using the Enzyme Kinetics Module of SigmaPlot. The data more closely followed positive cooperative kinetics ($n = 2.1$) as defined by the Hill equation ($R^2 = 0.95$) when compared with saturation kinetics as defined by the Michaelis-Menten equation ($R^2 = 0.89$). Maximum activity was observed at 4.9 mol%, and an analysis of the data according to the Hill equation yielded V_{max} and K_m values of 1,100 nmol/min/mg and 0.65 mol%, respectively. Overall, these data demonstrated that the enzyme operates in the scooting mode.

DISCUSSION

The *PAH1*-encoded Mg^{2+}-dependent PA phosphatase has emerged as a key enzyme whose activity controls the metabolism of lipids emanating from PA (Fig. 1) (5, 6, 11). The classic approach of measuring yeast PA phosphatase activity involves the incorporation of the substrate PA into a uniform Triton X-100/PA-mixed micelle (3, 93, 108). Although this detergent/phospholipid mixed micelle system has permitted defined activity measurements and studies to assess biochemical mechanisms of regulation (1, 64–66, 68, 93, 95, 96, 112), it lacks the mimicry of a biological membrane phospholipid bilayer. Here, we developed a liposome system, a widely accepted mimic of a biological membrane (99, 113, 114), to measure the activity of Pah1 PA phosphatase. To approximate the nuclear/ER membrane where the PA phosphatase catalyzes its reaction, the substrate PA was incorporated into liposomes comprised of PC/PE/PI/PS. These vesicles afforded a level of PA phosphatase activity greater to that obtained with the Triton X-100/PA-mixed micellar system (Fig. 4). As described previously (104), a simpler liposome composition (e.g., PC/PA) supported PA phosphatase activity, but at a much reduced level when compared with that observed with Triton X-100/PA-mixed micelles or with PA incorporated into the complex mixture of phospholipids. The reduced activity observed with PC/PA liposomes relative to that with Triton X-100/PA-mixed micelles has been attributed to the inability of the enzyme to access substrate at the inner leaflet of the vesicle membrane (104). Whereas this explanation is reasonable, the work presented here demonstrates that PA phosphatase activity is dependent on the phospholipid composition of the liposomes; a complex composition approximating that found in vivo yielded a robust level of activity (Fig. 5). The complex mixture of PC/PE/PI/PS/CDP-DAG, approximating the nuclear/ER membrane, also supports robust activity of the yeast phospholipid synthesis enzymes PI synthase (115) and PS synthase (116).

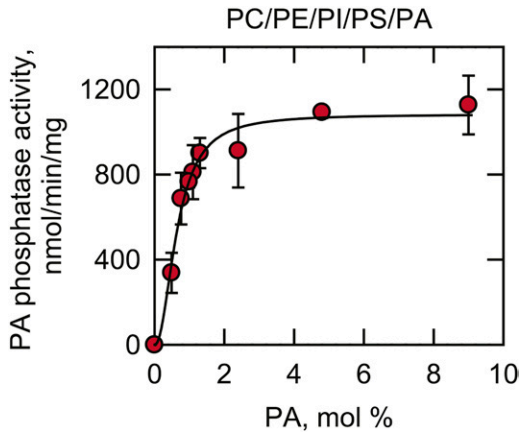

Fig. 9. Dependence of Pah1 PA phosphatase activity on the surface concentration of PA using liposomes composed of PC/PE/PI/PS/PA. Pah1 (80 ng) was assayed (15 min) for PA phosphatase activity by following the release of P_i from PA using PC/PE/PI/PS/PA liposomes with the indicated surface concentrations of PA. The molar concentration of PA was held constant at 1 mM and the total concentration of the PC/PE/PI/PS mixture was varied to obtain the indicated surface concentrations of PA. The best-fit curve is the result of a Hill analysis of the data using the Enzyme Kinetics module of SigmaPlot software.

The dependence of PA phosphatase activity on the phospholipid composition of liposomes was not governed by differences in the interaction of the enzyme with the vesicles; enzyme interaction was largely unaffected by the type and complexity of the phospholipids in PA-containing liposomes (Fig. 3). Whereas PA was not required for enzyme interaction with the liposomes composed of PC/PE/PI/PS, its presence afforded 60% greater interaction (Fig. 3). A similar situation has previously been shown with simple PC/PA liposomes (104) and with Triton X-100/PA-mixed micelles (93). While we did not examine the effect of PA fatty-acyl composition on enzyme-liposome interaction, the acyl composition of PA did not majorly affect the activity of the enzyme in liposomes composed of PC/PE/PI/PS/PA (Fig. 6). Whether the fatty-acyl content of PC, PE, PI, or PS would have an effect on PA phosphatase activity or enzyme-liposome interaction is unknown. The system developed here will permit additional studies to examine these questions, as well as whether other membrane lipids, such as CDP-DAG (96), and sphingoid bases (94), which have been shown to modulate PA phosphatase activity in Triton X-100/PA-mixed micelles, regulate the activity in liposomes. In our studies, we also observed that PA phosphatase activity depends on liposome size; greater activity was observed with large liposomes (e.g., 100 and 300 nm) when

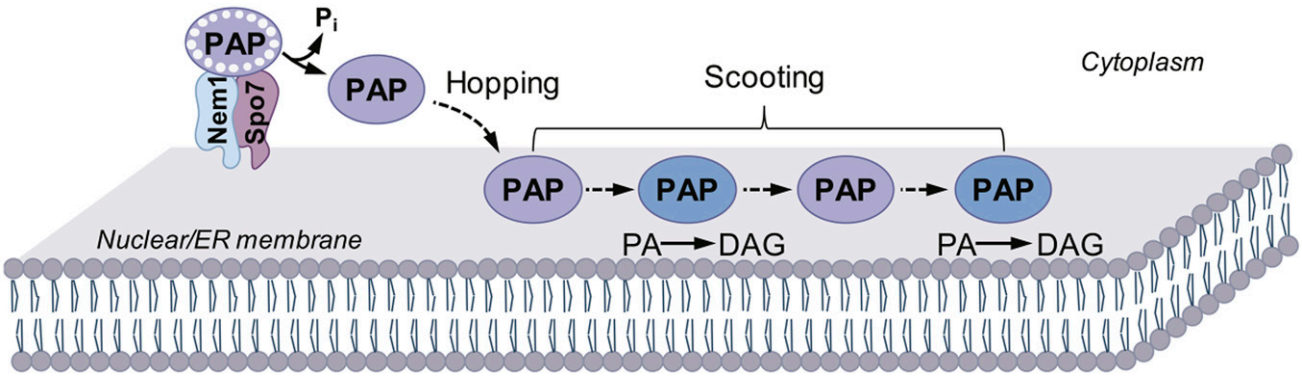

Fig. 10. Model for the action of Pah1 PA phosphatase (PAP) at the nuclear/ER membrane via the hopping and scooting modes. The phosphorylated form of PA phosphatase (small white circles) is dephosphorylated by the Nem1-Spo7 complex at the nuclear/ER membrane. The dephosphorylated PA phosphatase then hops onto the membrane surface. It then scoots along the membrane, binds to its substrate PA, and catalyzes the dephosphorylation of PA to produce DAG. Following the reaction, PA phosphatase scoots along the membrane until it binds another PA molecule. It then catalyzes the dephosphorylation of this PA to produce DAG. The PA phosphatase molecule catalyzing the dephosphorylation of PA is denoted with blue color.

compared with small liposomes (50 nm). This raised the suggestion that the PA phosphatase activity is sensitive to membrane phospholipid curvature (Fig. 7) (117).

The mammalian lipin 1, 2, and 3 isoforms of PA phosphatase have also been measured with PA incorporated into liposomes (54, 118–120). For these enzymes, the activity is augmented by the di-anionic form of PA, which is favored by a much elevated PE content (e.g., 60 mol%) in PC/PA liposomes (119, 120). Recognition of di-anionic PA is governed by the polybasic domains in the lipin proteins; phosphorylation prevents PA recognition for lipins 1 and 2, but has no effect for lipin 3 (119, 120). The yeast PA phosphatase does not possess a polybasic domain, and its activity is not regulated by PE (at least in detergent micelles (96)) or the ionic nature of PA (G-S. Han and G. M. Carman, unpublished observations). Nonetheless, the liposomes used to measure the lipin PA phosphatase enzymes do not approximate the membrane phospholipid composition in mammalian cells.

Whereas the impetus for this work was to develop an assay for the measurement of PA phosphatase activity in an environment that mimics the phospholipid composition of the nuclear/ER membrane, it also provided information on how the enzyme operates at the membrane. That PA phosphatase activity was dependent on the bulk concentration of PA in the PC/PE/PI/PS/PA liposomes (Fig. 5) indicated that the enzyme operates in the hopping mode (**Fig. 10**) (110). The kinetic analysis with the PC/PE/PI/PS/PA liposomes demonstrated that PA phosphatase activity was dependent on the surface concentration of PA (Fig. 9), and thus the enzyme also operates in the scooting mode (Fig. 10) (110). The surface K_m value for PA of 0.65 mol% is within, if not below, the physiological concentration (105, 106). Thus, small changes in the surface concentration of PA would have a major effect on the PA phosphatase activity at the nuclear/ER membrane. The enzyme activity exhibited cooperative kinetics with respect to the surface concentration of PA. Whether the Hill number of 2 reflects cooperative binding of two enzyme molecules or two substrate molecules is unclear and warrants additional studies. Owing that Pah1 appears to be monomeric (3), we favor a model by which the binding to one PA molecule facilitates interaction with a second substrate molecule. Precedence for such a mechanism (e.g., dual phospholipid model) comes from studies on the action of phospholipase A_2 toward phospholipid substrates (82, 84, 85, 111).

According to the model shown in Fig. 10, following its dephosphorylation by the Nem1-Spo7 protein phosphatase complex, the Pah1 PA phosphatase enzyme hops onto the membrane surface. This process, which is dependent on the amphipathic helix found at the N terminus (70), is facilitated by the presence of PA in the nuclear/ER membrane (70). After membrane interaction and binding to PA, the enzyme catalyzes its reaction to produce DAG. Following the reaction, the enzyme remains on the membrane surface and scoots along to bind another molecule of PA and carry out another round of catalysis. One would expect that it is more efficient for PA phosphatase to operate in the scooting mode as opposed to hopping from membrane surface to membrane surface to bind to its substrate PA (110). Yet, PA phosphatase operating in the hopping mode might be physiologically important in the context that the enzyme is reported to associate with membranes other than the nuclear/ER membrane. For example, Pah1 is also found at the nuclear vacuolar junction (121), the inner nuclear membrane (122), and in the vicinity of lipid droplets (123, 124). The phosphorylated form of Pah1 must be recruited to the nuclear/ER-associated Nem1-Spo7 complex for its dephosphorylation before membrane association and PA binding can occur (70). The ability of the unphosphorylated enzyme to operate in the hopping mode would permit its association with multiple membrane locations, especially if spatially close through organelle contact sites. In fact, a change in cell physiology (e.g., accelerated lipid droplet formation) might be a trigger for the enzyme to switch to its hopping mode of action. Testing this notion would benefit from the identification and mutation of specific residues required for the hopping and scooting modes of the enzyme.

Pah1 PA phosphatase is known to associate with the membrane for its cellular function through the control of the nuclear/ER membrane-associated Nem1-Spo7 phosphatase (41); its dephosphorylation by the phosphatase complex is essential for its membrane localization and catalytic function (32, 69, 123). In future studies, we will reconstitute the protein phosphatase complex into liposomes to examine the regulation of recruitment and dephosphorylation of Pah1 followed by the enzymatic dephosphorylation of PA in this defined model system.

Data availability

All data are contained within the article.

The authors thank Gil-Soo Han for providing the Pah1 used in the enzyme-liposome interactions studies, helpful discussions during the course of this work, and for comments in the preparation of the manuscript. The authors also acknowledge Edward A. Dennis for comments during the initial stages of the work.

REFERENCES

1. Han, G-S., W-I. Wu, and G. M. Carman. 2006. The *Saccharomyces cerevisiae* lipin homolog is a Mg^{2+}-dependent phosphatidate phosphatase enzyme. *J. Biol. Chem.* **281:** 9210–9218.
2. Smith, S. W., S. B. Weiss, and E. P. Kennedy. 1957. The enzymatic dephosphorylation of phosphatidic acids. *J. Biol. Chem.* **228:** 915–922.
3. Lin, Y-P., and G. M. Carman. 1989. Purification and characterization of phosphatidate phosphatase from *Saccharomyces cerevisiae*. *J. Biol. Chem.* **264:** 8641–8645.
4. Carman, G. M., and G. S. Han. 2018. Phosphatidate phosphatase regulates membrane phospholipid synthesis via phosphatidylserine synthase. *Adv. Biol. Regul.* **67:** 49–58.
5. Carman, G. M., and G. S. Han. 2019. Fat-regulating phosphatidic acid phosphatase: a review of its roles and regulation in lipid homeostasis. *J. Lipid Res.* **60:** 2–6.
6. Kwiatek, J. M., G. S. Han, and G. M. Carman. 2020. Phosphatidate-mediated regulation of lipid synthesis at the nuclear/endoplasmic reticulum membrane. *Biochim. Biophys. Acta Mol. Cell Biol. Lipids.* **1865:** 158434.
7. Carman, G. M., and S. A. Henry. 1989. Phospholipid biosynthesis in yeast. *Annu. Rev. Biochem.* **58:** 635–669.
8. Carman, G. M., and G. M. Zeimetz. 1996. Regulation of phospholipid biosynthesis in the yeast *Saccharomyces cerevisiae*. *J. Biol. Chem.* **271:** 13293–13296.
9. Carman, G. M., and S. A. Henry. 1999. Phospholipid biosynthesis in the yeast *Saccharomyces cerevisiae* and interrelationship with other metabolic processes. *Prog. Lipid Res.* **38:** 361–399.
10. Carman, G. M., and G-S. Han. 2009. Regulation of phospholipid synthesis in yeast. *J. Lipid Res.* **50:** S69–S73.
11. Carman, G. M., and G-S. Han. 2011. Regulation of phospholipid synthesis in the yeast *Saccharomyces cerevisiae*. *Annu. Rev. Biochem.* **80:** 859–883.
12. Henry, S. A., S. Kohlwein, and G. M. Carman. 2012. Metabolism and regulation of glycerolipids in the yeast *Saccharomyces cerevisiae*. *Genetics.* **190:** 317–349.
13. Weiss, S. B., E. P. Kennedy, and J. Y. Kiyasu. 1960. The enzymatic synthesis of triglycerides. *J. Biol. Chem.* **235:** 40–44.
14. Czabany, T., K. Athenstaedt, and G. Daum. 2007. Synthesis, storage and degradation of neutral lipids in yeast. *Biochim. Biophys. Acta.* **1771:** 299–309.
15. Müllner, H., and G. Daum. 2004. Dynamics of neutral lipid storage in yeast. *Acta Biochim. Pol.* **51:** 323–347.
16. Sorger, D., and G. Daum. 2003. Triacylglycerol biosynthesis in yeast. *Appl. Microbiol. Biotechnol.* **61:** 289–299.
17. Aflaki, E., B. Radovic, P. G. Chandak, D. Kolb, T. Eisenberg, J. Ring, I. Fertschai, A. Uellen, H. Wolinski, S-D. Kohlwein, et al. 2011. Triacylglycerol accumulation activates the mitochondrial apoptosis pathway in macrophages. *J. Biol. Chem.* **286:** 7418–7428.
18. Kohlwein, S. D. 2010. Triacylglycerol homeostasis: insights from yeast. *J. Biol. Chem.* **285:** 15663–15667.
19. Petschnigg, J., H. Wolinski, D. Kolb, G. Zellnig, C. F. Kurat, K. Natter, and S. D. Kohlwein. 2009. Good fat - essential cellular requirements for triacylglycerol synthesis to maintain membrane homeostasis in yeast. *J. Biol. Chem.* **284:** 30981–30993.
20. Borkenhagen, L. F., and E. P. Kennedy. 1957. The enzymatic synthesis of cytidine diphosphate choline. *J. Biol. Chem.* **227:** 951–962.
21. Carter, J. R., and E. P. Kennedy. 1966. Enzymatic synthesis of cytidine diphosphate diglyceride. *J. Lipid Res.* **7:** 678–683.
22. Kennedy, E. P., and S. B. Weiss. 1956. The function of cytidine coenzyme in the biosynthesis of phospholipids. *J. Biol. Chem.* **222:** 193–214.
23. Kennedy, E. P. 1956. The synthesis of cytidine diphosphate choline, cytidine diphosphate ethanolamine, and related compounds. *J. Biol. Chem.* **222:** 185–191.
24. Weiss, S. B., S. W. Smith, and E. P. Kennedy. 1958. The enzymatic formation of lecithin from cytidine diphosphate choline and D-1,2-diglyceride. *J. Biol. Chem.* **231:** 53–64.
25. McMaster, C. R., and R. M. Bell. 1994. Phosphatidylcholine biosynthesis via the CDP-choline pathway in *Saccharomyces cerevisiae*. Multiple mechanisms of regulation. *J. Biol. Chem.* **269:** 14776–14783.
26. McDonough, V. M., R. J. Buxeda, M. E. C. Bruno, O. Ozier-Kalogeropoulos, M-T. Adeline, C. R. McMaster, R. M. Bell, and G. M. Carman. 1995. Regulation of phospholipid biosynthesis in *Saccharomyces cerevisiae* by CTP. *J. Biol. Chem.* **270:** 18774–18780.
27. Atkinson, K. D., B. Jensen, A. I. Kolat, E. M. Storm, S. A. Henry, and S. Fogel. 1980. Yeast mutants auxotropic for choline or ethanolamine. *J. Bacteriol.* **141:** 558–564.
28. Clancey, C. J., S-C. Chang, and W. Dowhan. 1993. Cloning of a gene (*PSD1*) encoding phosphatidylserine decarboxylase from *Saccharomyces cerevisiae* by complementation of an *Escherichia coli* mutant. *J. Biol. Chem.* **268:** 24580–24590.
29. Trotter, P. J., J. Pedretti, and D. R. Voelker. 1993. Phosphatidylserine decarboxylase from *Saccharomyces cerevisiae*. Isolation of mutants, cloning of the gene, and creation of a null allele. *J. Biol. Chem.* **268:** 21416–21424.
30. McGraw, P., and S. A. Henry. 1989. Mutations in the *Saccharomyces cerevisiae OPI3* gene: Effects on phospholipid methylation, growth, and cross pathway regulation of phospholipid synthesis. *Genetics.* **122:** 317–330.
31. Summers, E. F., V. A. Letts, P. McGraw, and S. A. Henry. 1988. *Saccharomyces cerevisiae cho2* mutants are deficient in phospholipid methylation and cross-pathway regulation of inositol synthesis. *Genetics.* **120:** 909–922.
32. Santos-Rosa, H., J. Leung, N. Grimsey, S. Peak-Chew, and S. Siniossoglou. 2005. The yeast lipin Smp2 couples phospholipid biosynthesis to nuclear membrane growth. *EMBO J.* **24:** 1931–1941.
33. Han, G-S., and G. M. Carman. 2017. Yeast *PAH1*-encoded phosphatidate phosphatase controls the expression of *CHO1*-encoded phosphatidylserine synthase for membrane phospholipid synthesis. *J. Biol. Chem.* **292:** 13230–13242.
34. Kudo, S., H. Shiino, S. Furuta, and Y. Tamura. 2020. Yeast transformation stress, together with loss of Pah1, phosphatidic acid phosphatase, leads to Ty1 retrotransposon insertion into the INO4 gene. *FASEB J.* **34:** 4749–4763.
35. Carman, G. M., and S. A. Henry. 2007. Phosphatidic acid plays a central role in the transcriptional regulation of glycerophospholipid synthesis in *Saccharomyces cerevisiae*. *J. Biol. Chem.* **282:** 37293–37297.
36. Dey, P., W. M. Su, G. S. Han, and G. M. Carman. 2017. Phosphorylation of lipid metabolic enzymes by yeast Pkc1 protein kinase C requires phosphatidylserine and diacylglycerol. *J. Lipid Res.* **58:** 742–751.
37. Pascual, F., A. Soto-Cardalda, and G. M. Carman. 2013. *PAH1*-encoded phosphatidate phosphatase plays a role in the growth phase- and inositol-mediated regulation of lipid synthesis in *Saccharomyces cerevisiae*. *J. Biol. Chem.* **288:** 35781–35792.
38. Adeyo, O., P. J. Horn, S. Lee, D. D. Binns, A. Chandrahas, K. D. Chapman, and J. M. Goodman. 2011. The yeast lipin orthologue Pah1p is important for biogenesis of lipid droplets. *J. Cell Biol.* **192:** 1043–1055.

39. Fakas, S., Y. Qiu, J. L. Dixon, G-S. Han, K. V. Ruggles, J. Garbarino, S. L. Sturley, and G. M. Carman. 2011. Phosphatidate phosphatase activity plays a key role in protection against fatty acid-induced toxicity in yeast. *J. Biol. Chem.* **286:** 29074–29085.
40. Park, Y., G. S. Han, E. Mileykovskaya, T. A. Garrett, and G. M. Carman. 2015. Altered lipid synthesis by lack of yeast Pah1 phosphatidate phosphatase reduces chronological life span. *J. Biol. Chem.* **290:** 25382–25394.
41. Siniossoglou, S., H. Santos-Rosa, J. Rappsilber, M. Mann, and E. Hurt. 1998. A novel complex of membrane proteins required for formation of a spherical nucleus. *EMBO J.* **17:** 6449–6464.
42. Han, G-S., S. Siniossoglou, and G. M. Carman. 2007. The cellular functions of the yeast lipin homolog Pah1p are dependent on its phosphatidate phosphatase activity. *J. Biol. Chem.* **282:** 37026–37035.
43. Hassaninasab, A., G-S. Han, and G. M. Carman. 2017. Tips on the analysis of phosphatidic acid by the fluorometric coupled enzyme assay. *Anal. Biochem.* **526:** 69–70.
44. Sasser, T., Q. S. Qiu, S. Karunakaran, M. Padolina, A. Reyes, B. Flood, S. Smith, C. Gonzales, and R. A. Fratti. 2012. The yeast lipin 1 orthologue Pah1p regulates vacuole homeostasis and membrane fusion. *J. Biol. Chem.* **287:** 2221–2236.
45. Xu, X., and K. Okamoto. 2018. The Nem1-Spo7 protein phosphatase complex is required for efficient mitophagy in yeast. *Biochem. Biophys. Res. Commun.* **496:** 51–57.
46. Rahman, M. A., M. G. Mostofa, and T. Ushimaru. 2018. The Nem1/Spo7-Pah1/lipin axis is required for autophagy induction after TORC1 inactivation. *FEBS J.* **285:** 1840–1860.
47. Lussier, M., A. M. White, J. Sheraton, T. di Paolo, J. Treadwell, S. B. Southard, C. I. Horenstein, J. Chen-Weiner, A. F. Ram, J. C. Kapteyn, et al. 1997. Large scale identification of genes involved in cell surface biosynthesis and architecture in *Saccharomyces cerevisiae*. *Genetics.* **147:** 435–450.
48. Ruiz, C., V. J. Cid, M. Lussier, M. Molina, and C. Nombela. 1999. A large-scale sonication assay for cell wall mutant analysis in yeast. *Yeast.* **15:** 1001–1008.
49. Irie, K., M. Takase, H. Araki, and Y. Oshima. 1993. A gene, *SMP2*, involved in plasmid maintenance and respiration in *Saccharomyces cerevisiae* encodes a highly charged protein. *Mol. Gen. Genet.* **236:** 283–288.
50. Córcoles-Sáez, I., M. L. Hernández, J. M. Martínez-Rivas, J. A. Prieto, and F. Randez-Gil. 2016. Characterization of the *S. cerevisiae* inp51 mutant links phosphatidylinositol 4,5-bisphosphate levels with lipid content, membrane fluidity and cold growth. *Biochim. Biophys. Acta.* **1861:** 213–226.
51. Han, G-S., L. O'Hara, G. M. Carman, and S. Siniossoglou. 2008. An unconventional diacylglycerol kinase that regulates phospholipid synthesis and nuclear membrane growth. *J. Biol. Chem.* **283:** 20433–20442.
52. Han, G-S., L. O'Hara, S. Siniossoglou, and G. M. Carman. 2008. Characterization of the yeast *DGK1*-encoded CTP-dependent diacylglycerol kinase. *J. Biol. Chem.* **283:** 20443–20453.
53. Péterfy, M., J. Phan, P. Xu, and K. Reue. 2001. Lipodystrophy in the *fld* mouse results from mutation of a new gene encoding a nuclear protein, lipin. *Nat. Genet.* **27:** 121–124.
54. Donkor, J., M. Sariahmetoglu, J. Dewald, D. N. Brindley, and K. Reue. 2007. Three mammalian lipins act as phosphatidate phosphatases with distinct tissue expression patterns. *J. Biol. Chem.* **282:** 3450–3457.
55. Han, G-S., and G. M. Carman. 2010. Characterization of the human *LPIN1*-encoded phosphatidate phosphatase isoforms. *J. Biol. Chem.* **285:** 14628–14638.
56. Nadra, K., A-S. de Preux Charles, J-J. Medard, W. T. Hendriks, G-S. Han, S. Grès, G. M. Carman, J-S. Saulnier-Blache, M. H. G. Verheijen, and R. Chrast. 2008. Phosphatidic acid mediates demyelination in *Lpin1* mutant mice. *Genes Dev.* **22:** 1647–1661.
57. Zeharia, A., A. Shaag, R. H. Houtkooper, T. Hindi, P. de Lonlay, G. Erez, L. Hubert, A. Saada, Y. de Keyzer, G. Eshel, et al. 2008. Mutations in *LPIN1* cause recurrent acute myoglobinuria in childhood. *Am. J. Hum. Genet.* **83:** 489–494.
58. Donkor, J., P. Zhang, S. Wong, L. O'Loughlin, J. Dewald, B. P. C. Kok, D. N. Brindley, and K. Reue. 2009. A conserved serine residue is required for the phosphatidate phosphatase activity but not transcriptional coactivator functions of lipin-1 and lipin-2. *J. Biol. Chem.* **284:** 29968–29978.
59. Zhang, P., M. A. Verity, and K. Reue. 2014. Lipin-1 regulates autophagy clearance and intersects with statin drug effects in skeletal muscle. *Cell Metab.* **20:** 267–279.
60. Wiedmann, S., M. Fischer, M. Koehler, K. Neureuther, G. Riegger, A. Doering, H. Schunkert, C. Hengstenberg, and A. Baessler. 2008. Genetic variants within the *LPIN1* gene, encoding lipin, are influencing phenotypes of the metabolic syndrome in humans. *Diabetes.* **57:** 209–217.
61. Mul, J. D., K. Nadra, N. B. Jagalur, I. J. Nijman, P. W. Toonen, J-J. Médard, S. Grès, A. de Bruin, G-S. Han, J. F. Brouwers, et al. 2011. A hypomorphic mutation in *Lpin1* induces progressively improving neuropathy and lipodystrophy in the rat. *J. Biol. Chem.* **286:** 26781–26793.
62. Reue, K., and H. Wang. 2019. Mammalian lipin phosphatidic acid phosphatases in lipid synthesis and beyond: metabolic and inflammatory disorders. *J. Lipid Res.* **60:** 728–733.
63. Choi, H-S., W-M. Su, J. M. Morgan, G-S. Han, Z. Xu, E. Karanasios, S. Siniossoglou, and G. M. Carman. 2011. Phosphorylation of phosphatidate phosphatase regulates its membrane association and physiological functions in *Saccharomyces cerevisiae:* identification of Ser^{602}, Thr^{723}, and Ser^{744} as the sites phosphorylated by *CDC28* (*CDK1*)-encoded cyclin-dependent kinase. *J. Biol. Chem.* **286:** 1486–1498.
64. Choi, H-S., W-M. Su, G-S. Han, D. Plote, Z. Xu, and G. M. Carman. 2012. Pho85p-Pho80p phosphorylation of yeast Pah1p phosphatidate phosphatase regulates its activity, location, abundance, and function in lipid metabolism. *J. Biol. Chem.* **287:** 11290–11301.
65. Su, W-M., G-S. Han, J. Casciano, and G. M. Carman. 2012. Protein kinase A-mediated phosphorylation of Pah1p phosphatidate phosphatase functions in conjunction with the Pho85p-Pho80p and Cdc28p-cyclin B kinases to regulate lipid synthesis in yeast. *J. Biol. Chem.* **287:** 33364–33376.
66. Su, W-M., G-S. Han, and G. M. Carman. 2014. Cross-talk phosphorylations by protein kinase C and Pho85p-Pho80p protein kinase regulate Pah1p phosphatidate phosphatase abundance in *Saccharomyces cerevisiae*. *J. Biol. Chem.* **289:** 18818–18830.
67. Hsieh, L-S., W-M. Su, G-S. Han, and G. M. Carman. 2016. Phosphorylation of yeast Pah1 phosphatidate phosphatase by casein kinase II regulates its function in lipid metabolism. *J. Biol. Chem.* **291:** 9974–9990.
68. Hassaninasab, A., L. S. Hsieh, W. M. Su, G. S. Han, and G. M. Carman. 2019. Yck1 casein kinase I regulates the activity and phosphorylation of Pah1 phosphatidate phosphatase from *Saccharomyces cerevisiae*. *J. Biol. Chem.* **294:** 18256–18268.
69. O'Hara, L., G-S. Han, S. Peak-Chew, N. Grimsey, G. M. Carman, and S. Siniossoglou. 2006. Control of phospholipid synthesis by phosphorylation of the yeast lipin Pah1p/Smp2p Mg^{2+}-dependent phosphatidate phosphatase. *J. Biol. Chem.* **281:** 34537–34548.
70. Karanasios, E., G-S. Han, Z. Xu, G. M. Carman, and S. Siniossoglou. 2010. A phosphorylation-regulated amphipathic helix controls the membrane translocation and function of the yeast phosphatidate phosphatase. *Proc. Natl. Acad. Sci. USA.* **107:** 17539–17544.
71. Carman, G. M. 2019. Discoveries of the phosphatidate phosphatase genes in yeast published in the *Journal of Biological Chemistry*. *J. Biol. Chem.* **294:** 1681–1689.
72. Su, W-M., G-S. Han, and G. M. Carman. 2014. Yeast Nem1-Spo7 protein phosphatase activity on Pah1 phosphatidate phosphatase is specific for the Pho85-Pho80 protein kinase phosphorylation sites. *J. Biol. Chem.* **289:** 34699–34708.
73. Pascual, F., L-S. Hsieh, A. Soto-Cardalda, and G. M. Carman. 2014. Yeast Pah1p phosphatidate phosphatase is regulated by proteasome-mediated degradation. *J. Biol. Chem.* **289:** 9811–9822.
74. Hsieh, L-S., W-M. Su, G-S. Han, and G. M. Carman. 2015. Phosphorylation regulates the ubiquitin-independent degradation of yeast Pah1 phosphatidate phosphatase by the 20S proteasome. *J. Biol. Chem.* **290:** 11467–11478.
75. Carman, G. M., and W. Dowhan. 1979. Phosphatidylserine synthase from *Escherichia coli*: the role of Triton X-100 in catalysis. *J. Biol. Chem.* **254:** 8391–8397.
76. Warner, T. G., and E. A. Dennis. 1975. Action of the highly purified, membrane-bound enzyme phosphatidylserine decarboxylase from *Escherichia coli* toward phosphatidylserine in mixed micelles and erythrocyte ghosts in the presence of surfactant. *J. Biol. Chem.* **250:** 8004–8009.

77. Bae-Lee, M., and G. M. Carman. 1990. Regulation of yeast phosphatidylserine synthase and phosphatidylinositol synthase activities by phospholipids in Triton X-100/phospholipid mixed micelles. *J. Biol. Chem.* **265:** 7221–7226.
78. Fischl, A. S., and G. M. Carman. 1983. Phosphatidylinositol biosynthesis in *Saccharomyces cerevisiae*: purification and properties of microsome-associated phosphatidylinositol synthase. *J. Bacteriol.* **154:** 304–311.
79. Buxeda, R. J., J. T. Nickels, Jr., C. J. Belunis, and G. M. Carman. 1991. Phosphatidylinositol 4-kinase from *Saccharomyces cerevisiae*. Kinetic analysis using Triton X-100/phosphatidylinositol-mixed micelles. *J. Biol. Chem.* **266:** 13859–13865.
80. Wissing, J. B., B. Kornak, A. Funke, and B. Riedel. 1994. Phosphatidate kinase, a novel enzyme in phospholipid metabolism. Characterization of the enzyme from suspension-cultured *Catharanthus roseus* cells. *Plant Physiol.* **105:** 903–909.
81. Kucera, G. L., C. Miller, P. J. Sisson, R. W. Wilcox, Z. Wiemer, and M. Waite. 1988. Hydrolysis of thioester analogs by rat liver phospholipase A1. *J. Biol. Chem.* **263:** 12964–12969.
82. Roberts, M. F., R. A. Deems, and E. A. Dennis. 1977. Dual role of interfacial phospholipid in phospholipase A2 catalysis. *Proc. Natl. Acad. Sci. USA.* **74:** 1950–1954.
83. Dennis, E. A. 1973. Kinetic dependence of phospholipase A2 activity on the detergent Triton X-100. *J. Lipid Res.* **14:** 152–159.
84. Deems, R. A., B. R. Eaton, and E. A. Dennis. 1975. Kinetic analysis of phospholipase A2 activity toward mixed micelles and its implications for the study of lipolytic enzymes. *J. Biol. Chem.* **250:** 9013–9020.
85. Hendrickson, H. S., and E. A. Dennis. 1984. Kinetic analysis of the dual phospholipid model for phospholipase A2 action. *J. Biol. Chem.* **259:** 5734–5739.
86. Eaton, B. R., and E. A. Dennis. 1976. Analysis of phospholipase C (*Bacillus cereus*) action toward mixed micelles of phospholipid and surfactant. *Arch. Biochem. Biophys.* **176:** 604–609.
87. Sundler, R., A. W. Alberts, and P. R. Vagelos. 1978. Enzymatic properties of phosphatidylinositol inositolphosphohydrolase from *Bacillus cereus*. Substrate dilution in detergent-phospholipid micelles and bilayer vesicles. *J. Biol. Chem.* **253:** 4175–4179.
88. Qin, C., C. Wang, and X. Wang. 2002. Kinetic analysis of Arabidopsis phospholipase Ddelta. Substrate preference and mechanism of activation by Ca2+ and phosphatidylinositol 4,5-biphosphate. *J. Biol. Chem.* **277:** 49685–49690.
89. James, S. R., A. Paterson, T. K. Harden, and C. P. Downes. 1995. Kinetic analysis of phospholipase C beta isoforms using phospholipid-detergent mixed micelles. Evidence for interfacial catalysis involving distinct micelle binding and catalytic steps. *J. Biol. Chem.* **270:** 11872–11881.
90. Wu, W-I., Y. Liu, B. Riedel, J. B. Wissing, A. S. Fischl, and G. M. Carman. 1996. Purification and characterization of diacylglycerol pyrophosphate phosphatase from *Saccharomyces cerevisiae*. *J. Biol. Chem.* **271:** 1868–1876.
91. Chae, M., and G. M. Carman. 2013. Characterization of the yeast actin patch protein App1p phosphatidate phosphatase. *J. Biol. Chem.* **288:** 6427–6437.
92. Furneisen, J. M., and G. M. Carman. 2000. Enzymological properties of the *LPP1*-encoded lipid phosphatase from *Saccharomyces cerevisiae*. *Biochim. Biophys. Acta.* **1484:** 71–82.
93. Lin, Y-P., and G. M. Carman. 1990. Kinetic analysis of yeast phosphatidate phosphatase toward Triton X-100/phosphatidate mixed micelles. *J. Biol. Chem.* **265:** 166–170.
94. Wu, W-I., Y-P. Lin, E. Wang, A. H. Merrill, Jr., and G. M. Carman. 1993. Regulation of phosphatidate phosphatase activity from the yeast *Saccharomyces cerevisiae* by sphingoid bases. *J. Biol. Chem.* **268:** 13830–13837.
95. Wu, W-I., and G. M. Carman. 1994. Regulation of phosphatidate phosphatase activity from the yeast *Saccharomyces cerevisiae* by nucleotides. *J. Biol. Chem.* **269:** 29495–29501.
96. Wu, W-I., and G. M. Carman. 1996. Regulation of phosphatidate phosphatase activity from the yeast *Saccharomyces cerevisiae* by phospholipids. *Biochemistry.* **35:** 3790–3796.
97. Bradford, M. M. 1976. A rapid and sensitive method for the quantitation of microgram quantities of protein utilizing the principle of protein-dye binding. *Anal. Biochem.* **72:** 248–254.
98. Laemmli, U. K. 1970. Cleavage of structural proteins during the assembly of the head of bacteriophage T4. *Nature.* **227:** 680–685.
99. MacDonald, R. C., R. I. MacDonald, B. P. Menco, K. Takeshita, N. K. Subbarao, and L. R. Hu. 1991. Small-volume extrusion apparatus for preparation of large, unilamellar vesicles. *Biochim. Biophys. Acta.* **1061:** 297–303.
100. Guengerich, F. P., P. Wang, and N. K. Davidson. 1982. Estimation of isozymes of microsomal cytochrome P-450 in rats, rabbits, and humans using immunochemical staining coupled with sodium dodecyl sulfate-polyacrylamide gel electrophoresis. *Biochemistry.* **21:** 1698–1706.
101. Burnette, W. N. 1981. Western blotting: electrophoretic transfer of proteins from sodium dodecyl sulfate-polyacrylamide gels to unmodified nitrocellulose and radiographic detection with antibody and radioiodinated protein A. *Anal. Biochem.* **112:** 195–203.
102. Haid, A., and M. Suissa. 1983. Immunochemical identification of membrane proteins after sodium dodecyl sulfate-polyacrylamide gel electrophoresis. *Methods Enzymol.* **96:** 192–205.
103. Havriluk, T., F. Lozy, S. Siniossoglou, and G. M. Carman. 2008. Colorimetric determination of pure Mg^{2+}-dependent phosphatidate phosphatase activity. *Anal. Biochem.* **373:** 392–394.
104. Xu, Z., W-M. Su, and G. M. Carman. 2012. Fluorescence spectroscopy measures yeast *PAH1*-encoded phosphatidate phosphatase interaction with liposome membranes. *J. Lipid Res.* **53:** 522–528.
105. Rattray, J. B., A. Schibeci, and D. K. Kidby. 1975. Lipids of yeast. *Bacteriol. Rev.* **39:** 197–231.
106. Henry, S. A. 1982. Membrane lipids of yeast: biochemical and genetic studies. *In* The Molecular Biology of the Yeast Saccharomyces: Metabolism and Gene Expression. J. N. Strathern, E. W. Jones, and J. R. Broach, editors. Cold Spring Harbor Laboratory, Cold Spring Harbor, New York. 101–158.
107. Zinser, E., C. D. M. Sperka-Gottlieb, E-V. Fasch, S. D. Kohlwein, F. Paltauf, and G. Daum. 1991. Phospholipid synthesis and lipid composition of subcellular membranes in the unicellular eukaryote *Saccharomyces cerevisiae*. *J. Bacteriol.* **173:** 2026–2034.
108. Carman, G. M., and Y-P. Lin. 1991. Phosphatidate phosphatase from yeast. *Methods Enzymol.* **197:** 548–553.
109. Brot, F. E., and M. L. Bender. 1969. Use of the specificity constant of α-chymotrypsin. *J. Am. Chem. Soc.* **91:** 7187–7191.
110. Jain, M. K., and O. G. Berg. 1989. The kinetics of interfacial catalysis by phospholipase A_2 and regulation of interfacial activation: hopping versus scooting. *Biochim. Biophys. Acta.* **1002:** 127–156.
111. Carman, G. M., R. A. Deems, and E. A. Dennis. 1995. Lipid signaling enzymes and surface dilution kinetics. *J. Biol. Chem.* **270:** 18711–18714.
112. Wu, W-I., and G. M. Carman. 2000. Kinetic analysis of sphingoid base inhibition of yeast phosphatidate phosphatase. *Methods Enzymol.* **312:** 373–380.
113. Enoch, H. G., and P. Stritmatter. 1979. Formation and properties of 1000 A diameter, single-bilayer phospholipid vesicles. *Proc. Natl. Acad. Sci. USA.* **76:** 145–149.
114. Szoka, F., and D. Papahadjopoulos. 1980. Comparative properties and methods of preparation of lipid vesicles (liposomes). *Annu. Rev. Biophys. Bioeng.* **9:** 467–508.
115. Fischl, A. S., M. J. Homann, M. A. Poole, and G. M. Carman. 1986. Phosphatidylinositol synthase from *Saccharomyces cerevisiae*. Reconstitution, characterization, and regulation of activity. *J. Biol. Chem.* **261:** 3178–3183.
116. Hromy, J. M., and G. M. Carman. 1986. Reconstitution of *Saccharomyces cerevisiae* phosphatidylserine synthase into phospholipid vesicles. Modulation of activity by phospholipids. *J. Biol. Chem.* **261:** 15572–15576.
117. Wu, W. I., and D. R. Voelker. 2004. Reconstitution of phosphatidylserine transport from chemically defined donor membranes to phosphatidylserine decarboxylase 2 implicates specific lipid domains in the process. *J. Biol. Chem.* **279:** 6635–6642.
118. Martin, A., A. Gomez-Munoz, Z. Jamal, and D. N. Brindley. 1991. Characterization and assay of phosphatidate phosphatase. *Methods Enzymol.* **197:** 553–563.
119. Eaton, J. M., G. R. Mullins, D. N. Brindley, and T. E. Harris. 2013. Phosphorylation of lipin 1 and charge on the phosphatidic acid head group control its phosphatidic acid phosphatase activity and membrane association. *J. Biol. Chem.* **288:** 9933–9945.
120. Boroda, S., S. Takkellapati, R. T. Lawrence, S. W. Entwisle, J. M. Pearson, M. E. Granade, G. R. Mullins, J. M. Eaton, J. Villén, and T. E. Harris. 2017. The phosphatidic acid-binding, polybasic domain is responsible for the differences in the phosphoregulation of lipins 1 and 3. *J. Biol. Chem.* **292:** 20481–20493.

121. Barbosa, A. D., H. Sembongi, W-M. Su, S. Abreu, F. Reggiori, G. M. Carman, and S. Siniossoglou. 2015. Lipid partitioning at the nuclear envelope controls membrane biogenesis. *Mol. Biol. Cell.* **26:** 3641–3657.
122. Romanauska, A., and A. Kohler. 2018. The inner nuclear membrane Is a metabolically active territory that generates nuclear lipid droplets. *Cell.* **174:** 700–715.e18.
123. Karanasios, E., A. D. Barbosa, H. Sembongi, M. Mari, G-S. Han, F. Reggiori, G. M. Carman, and S. Siniossoglou. 2013. Regulation of lipid droplet and membrane biogenesis by the acidic tail of the phosphatidate phosphatase Pah1p. *Mol. Biol. Cell.* **24:** 2124–2133.
124. Wolinski, H., H. F. Hofbauer, K. Hellauer, A. Cristobal-Sarramian, D. Kolb, M. Radulovic, O. L. Knittelfelder, G. N. Rechberger, and S. D. Kohlwein. 2015. Seipin is involved in the regulation of phosphatidic acid metabolism at a subdomain of the nuclear envelope in yeast. *Biochim. Biophys. Acta.* **1851:** 1450–1464.